© 2019. Published by The Company of Biologists Ltd | Journal of Experimental Biology (2019) 222, jeb210252. doi:10.1242/jeb.210252

RESEARCH ARTICLE

Dynamic relationship between noseleaf and pinnae in echolocating hipposiderid bats

Shuxin Zhang[1,2], Yanming Liu[1,3], Joanne Tang[2], Luoxiao Ying[4] and Rolf Müller[1,2,*]

ABSTRACT

Old World leaf-nosed bats (family Hipposideridae) can deform the shapes of their 'noseleaves' (i.e. ultrasonic emission baffles) and outer ears during echolocation behaviors. Prior work has shown that deformations on the emission as well as on the reception side can have an impact on the properties of the emitted/received sonar signals. The occurrence of the deformations on the emission and reception sides raises the question of whether the bats coordinate these two dynamic biosonar features to achieve synergistic effects. To address this question, simultaneous three-dimensional reconstructions of the trajectories of landmarks on the dynamic noseleaf and pinna geometries have been obtained in great roundleaf bats (*Hipposideros pratti*). These joint kinematics data on the noseleaf and pinnae have shown both qualitative and quantitative relationships between the noseleaf and pinna motions: large noseleaf deformations (opening or closing) tended to be associated with non-rigid pinna motions. Furthermore, closing deformations of the noseleaves tended to co-occur with closing motions of the pinna. Finally, a canonical correlation analysis of the motion trajectories has revealed a tight correlation between the motions of the landmarks on the noseleaf and both pinnae. These results demonstrate that the biosonar system of hipposiderid bats includes coordinated emission and reception dynamics.

KEY WORDS: Hipposiderid bats, Biosonar dynamics, Coordination of emission and reception dynamics

INTRODUCTION

Most laryngeally echolocating bats orient and hunt in complex environments such as dense vegetation (Neuweiler, 2000; Corcoran and Moss, 2017; Neuweiler et al., 1987). This requires considerable motor skills, e.g. maneuverability, as well as sensing capabilities that encode the relevant sensory information in a reliable fashion even in the presence of numerous nuisance echoes ('clutter'). The sensing capabilities involving prey in dense clutter in some bats are based on Doppler signatures (Schnitzler, 1968, 1973; Trappe and Schnitzler, 1982; Hiryu et al., 2005). Specifically, species in the families Rhinolophidae, Hipposideridae, Rhinonycteridae and a few species of Mormoopidae have an integrated system that includes adaptations in pulse design (Simmons and Stein, 1980; Bates et al., 2011; Matsuta et al., 2013), inner ear (Kössl and Vater, 1995; Davies et al., 2013), auditory system (Fujita and Kashimori, 2016; Moss and Sinha, 2003; Moss, 2018) and behavior (Commins, 2018; Yu et al., 2019; Simmons et al., 1979). But how do these species deal with the other sensing challenges, associated with orientation in clutter?

Peripheral dynamics in the biosonar systems of bats that exploit clutter could underlie the biosonar systems of these bats. Rhinolophids and hipposiderids emit their biosonar sounds through nostrils surrounded by elaborate noseleaves that diffract outgoing pulse waves (Metzner and Müller, 2016). Beyond their considerable geometric complexity, the noseleaves make fast changes in shape that coincide with signal emission (Feng et al., 2012). Numerical and physical methods indicate that noseleaf motions should impact the distribution of the emitted energy over direction (beam patterns) (He et al., 2015; Gupta et al., 2015; Fu et al., 2016). Rhinolophids and hipposiderids execute rigid and non-rigid pinna motions (Yin et al., 2017) accomplished by highly differentiated ear musculature (Schneider and Möhres, 1960). Experiments with robotic models have demonstrated target direction clues generated by rigid motions (Walker et al., 1998), and numerical predictions have shown changes in the nature of the beam patterns in response to non-rigid pinna motions (Gao et al., 2011). Data from robotic models and numerical simulations reveal that beam pattern changes owing to non-rigid noseleaf and pinna motions can lead to encoding additional sensory information that improve direction-finding performance (Müller et al., 2017; Gupta et al., 2018). Bats with surgically destroyed pinna mobility do not perform well in obstacle avoidance trials (Mogdans et al., 1988). Our underlying hypothesis is that movements of noseleaf and pinnae are important to biosonar performance of rhinolophid and hipposiderid bats.

First, we tested the prediction that noseleaf and pinnae motions during echolocation are coordinated. If noseleaf and pinna motions have independent impacts on the sensory performance, there need be no coordination. Alternatively, coordination of dynamics on the signal emission and reception could enhance the sensory performance. At present, it remains to be seen whether such synergies exist and what the underlying mechanism could be.

To test the prediction that there is coordination between emission and reception, we affixed landmark points on the noseleaf and both pinnae. We simultaneously used high-speed stereo vision to document the bats' behavior. We used categorizations of movements of pinnae and noseleaf combined with canonical correlation. If movements of the pinnae and noseleaf are coordinated, we would expect that a given noseleaf motion type would coincide more frequently with certain pinna motion types. We also expected that canonical correlation would detect a relationship between the motions. But, a negative result of either analysis does not reject the hypothesis, because neither method is guaranteed to find any existing relationship. By demonstrating coordination between emission and

[1]Shandong University-Virginia Tech International Laboratory, School of Physics, Shandong University, Jinan 250100, China. [2]Department of Mechanical Engineering, Virginia Tech, Blacksburg, VA 24061, USA. [3]School of Mechanical Engineering, Shandong University, Jinan 250061, China. [4]School of Electrical Engineering, Shandong University, Jinan 250002, China.

*Author for correspondence (rolf.mueller@vt.edu)

S.Z., 0000-0001-5352-8958; Y.L., 0000-0001-7400-6374; J.T., 0000-0002-6926-4341; L.Y., 0000-0003-3175-0579; R.M., 0000-0001-8358-4053

Received 9 July 2019; Accepted 29 August 2019

Journal of Experimental Biology (2019) 222, jeb210252. doi:10.1242/jeb.210252

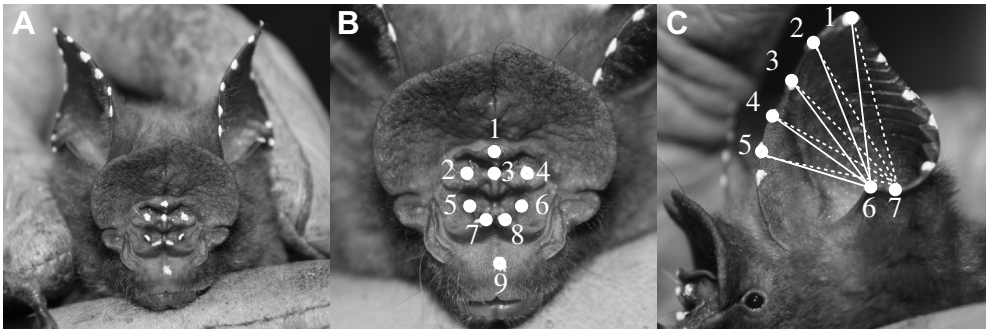

Fig. 1. Tracking of landmarks on the noseleaf and pinna. (A) Male individual of Pratt's roundleaf bat (*Hipposideros pratti*) with landmarks on the noseleaf and pinna. (B) Noseleaf landmark pattern analyzed in the present study. (C) Pinna landmarks and distances between them that were evaluated here.

reception dynamics, a positive result of this analysis could lay the foundation for a better understanding of active, dynamic sensing paradigms in bats and beyond.

MATERIALS AND METHODS

We tested four adult male Pratt's leaf-nosed bats (*Hipposideros pratti* Thomas 1891; Fig. 1A) obtained from caves in two regions in southern China, Sha County in Fujian Province and Yongfeng County in Jiangxi Province. We kept the bats in a climate-controlled indoor flight room (length 6.9 m, width 1.3 m, height 3.2 m) at 22 and 25°C and 60–70% relative humidity. We kept the bats in a reverse 12 h:12 h light:dark cycle and worked with them in the dark. We fed the bats mealworms enriched with vitamin and mineral supplements and provided water *ad libitum*.

We exposed the bats to a variety of changing biosonar targets to attract their attention and elicit exploratory biosonar behaviors triggered by novelty. We presented scenarios that were recreations of natural targets in clutter, i.e. small foliage branches with leaves, as well as a small propeller to mimic the properties of echoes from a flying insect. We changed targets to minimize habituation and elicit noseleaf and pinna motion behaviors. All targets were presented at a distance of approximately 1 m from the animals.

All animal work complied with the Principles of Animal Care, publication no. 86-23, revised 1985, of the National Institutes of Health, and with the relevant guidelines and regulations of the People's Republic of China. All experiments were carried out under an institutional permit from the Animal Care Committee of the Shandong University–Virginia Tech International Laboratory that specifically approved the study.

Quantitative characterizations of the joint noseleaf and pinnae motions were obtained in the form of three-dimensional trajectories for landmarks (non-toxic white dye spots) on the noseleaf and pinna (Fig. 1) ahead of an experiment. All landmarks were washed off immediately after completion of the experimental session. At a minimum, a total of 23 landmark points were placed on each bat, nine on the noseleaf (Fig. 1B) and seven along the rim of each pinna (Fig. 1A,C). The positions of the landmark points were tracked with an array of four synchronized high-speed video cameras (GigaView, Southern Vision System Inc., Huntsville, AL, USA; frame rate 400 Hz, image resolution 800×600 pixels).

Before an experiment, all high-speed cameras were calibrated with a set of 25 images of a planar checkerboard to estimate the intrinsic parameters (including nonlinear distortion) of each camera as well as the relative positions and orientations of the cameras (Camera Calibration Toolbox for MATLAB, The MathWorks, Natick, MA,

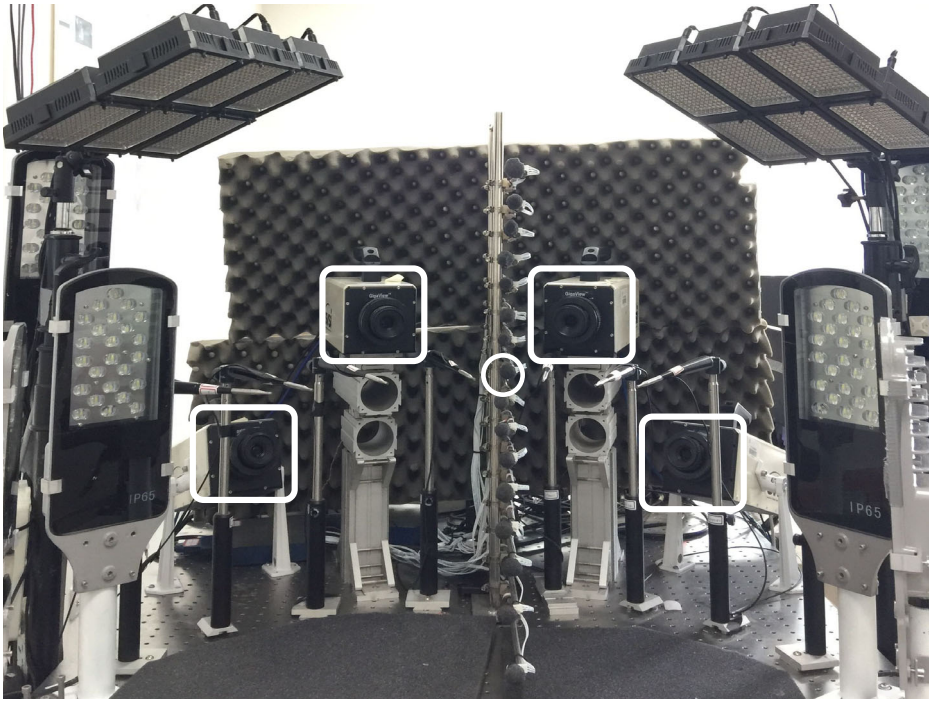

Fig. 2. Experimental setup. Four high-speed video cameras (marked by white squares) were used to record the three motion trajectories of the landmarks on the noseleaf and pinnae. An ultrasonic measurement microphone (white circle) was used to record the bats' ultrasonic pulses. Recordings from the cameras and the microphone were triggered simultaneously. Illumination was provided by six sets of LED lights (seen in the two upper image corners).

Journal of Experimental Biology (2019) 222, jeb210252. doi:10.1242/jeb.210252

USA; Bouguet and Perona, 1998). The two-dimensional image coordinates of the landmarks from at least two cameras were obtained by an automatic point-tracking algorithm based on iterative and multiple-pass cross-correlation and centroid identification (Hedrick, 2008). The three-dimensional coordinates of the landmark points were estimated through stereo triangulation (Bouguet and Perona, 1998). In the final step, the three-dimensional coordinates of all landmark points on the noseleaf and the pinnae were transformed into a unified world coordinate system regardless of which camera pair they were obtained from. This was done by translation and rotation based on the extrinsic parameters of the cameras.

A measurement microphone (1/8 inch pressure microphone, type 40 DP, G.R.A.S. Sound and Vibration, Holte, Denmark) was used to record the ultrasonic emissions from the bats during the experiments. The purpose of these recordings was to ensure that the analyzed high-speed video recordings were accompanied by biosonar pulse emissions. The microphone was mounted at the same height as the platform on which the bat was positioned at a distance of 35 cm in front of the animal (Fig. 2). A board of sound-proof foam was used to shield the microphone at the site opposite of the bat (Fig. 2). The microphone was calibrated with a sound level calibrator [type 4231, Brüel & Kjær, Nærum, Denmark, 114 dB sound pressure level (SPL) at 1 kHz]. The analog output signals of the measurement microphone were digitized at a sampling rate of 512 kHz and 16 bit resolution (PXIe-6358, RIO platform, National Instruments, Austin, TX, USA). The microphone and the high-speed cameras were triggered simultaneously with custom control software (written for the MATLAB environment).

A total of 112 continuous recording sequences, each with 3 s duration, i.e. 1200 high-speed video frames per camera for each sequence, were obtained. From these 112 recordings, 295 distinct noseleaf and pinna motion sequences were identified manually. To assess whether the recorded noseleaf motion data were homogeneous or contained distinct groups, all noseleaf motion sequences were submitted to clustering (*k*-means algorithm; Likas et al., 2003) based on the following features: (i) maximum change in noseleaf height

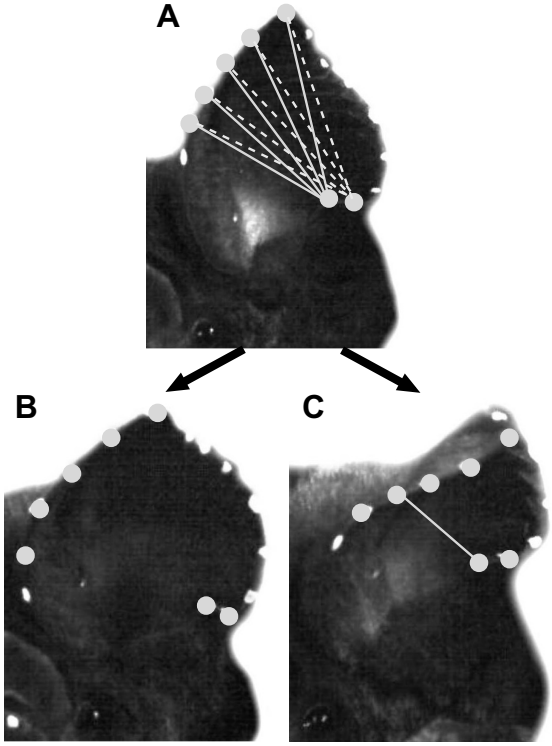

Fig. 3. Classification of rigid and non-rigid pinna motions. (A) Upright (initial) position of the pinna, (B) pinna after a rigid motion (forward rotation), (C) pinna after a non-rigid motion (closing deformation).

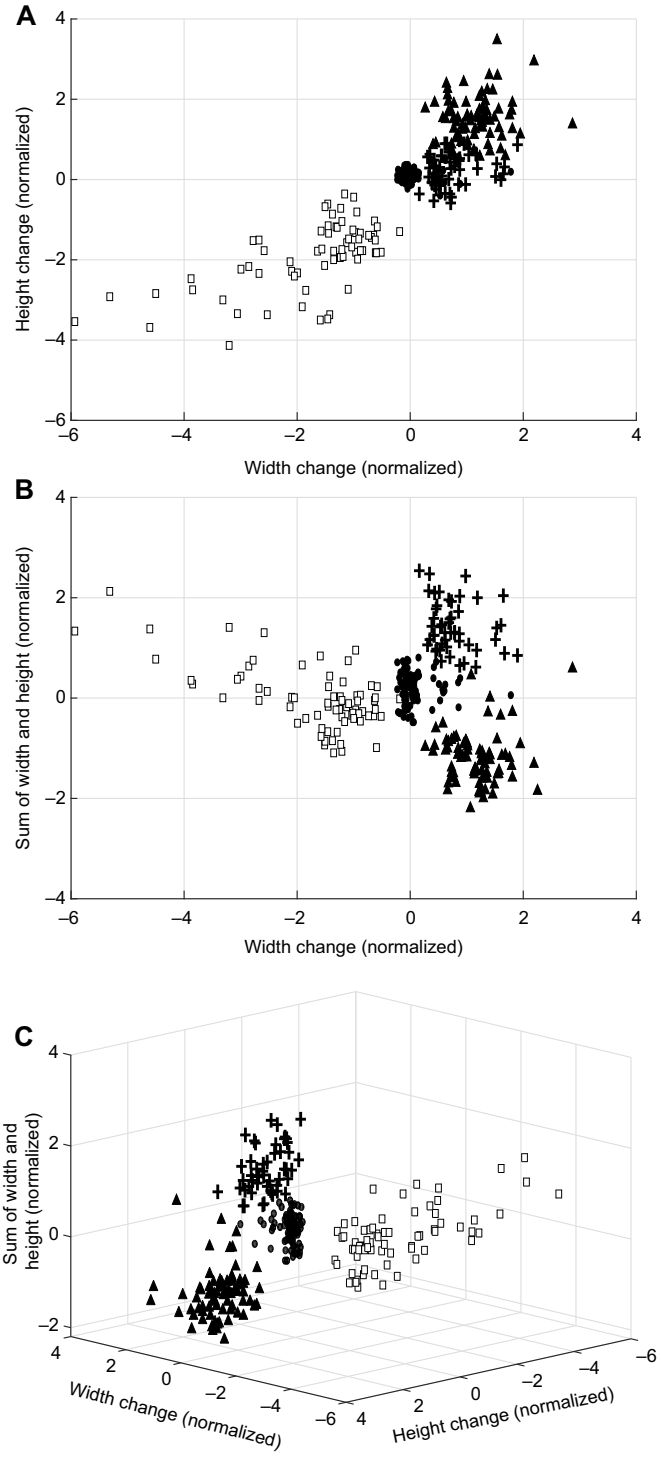

Fig. 4. Clusters found among the noseleaf motion recordings (*N*=295) in a space spanned by the changes in width and height and the sum of noseleaf width and height. Open squares, closing motions; filled triangles, opening motions; crosses: random motions; filled circles, no motion. The data were normalized along each dimension by the respective standard deviation. A–C show different viewing angles of the data distribution.

Journal of Experimental Biology (2019) 222, jeb210252. doi:10.1242/jeb.210252

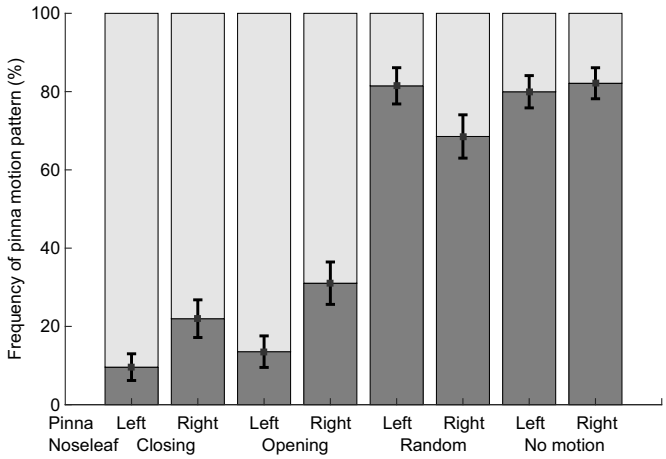

Fig. 5. Frequency of occurrence for rigid and non-rigid pinna motions across the four noseleaf motion types. For each noseleaf motion type, a pair of bars shows the relative frequencies of rigid (dark gray) and non-rigid (light gray) motion patterns for the left and right pinnae. Frequency estimates were based on noseleaf motion patterns; the filled circles and error bars represent the mean and standard deviation obtained from a set of 1000 bootstrap samples taken from this dataset.

over the entire noseleaf motion sequence, where noseleaf height was measured as the distance between point 3 and the midpoint of the line between points 7 and 8, i.e. it excluded the coronet and the secondary leaves (Fig. 1B); (ii) maximum change in noseleaf width over the entire motion sequence, where noseleaf width was measured as the distance between points 5 and 6 (Fig. 1B); and (iii) opening state (i.e. open or closed) of the noseleaf at the start of noseleaf motion sequence measured by the sum of noseleaf width and height as defined under (i) and (ii). In order to ensure that all features had equal weight in clustering, the experimental values for each of these three features were normalized by subtracting the mean and dividing by the standard deviation of the sample. The mean and standard deviation for each of the features were determined over the entire motion sequence dataset.

The pinna motions that occurred during the recordings were classified into two categories, 'rigid' and 'non-rigid' (Fig. 3), based on the maximum changes in the distances between all five landmark points during the motion. If the maximum change was less than 2 mm, the motion was classified as rigid, else it was classified as non-rigid (Yin et al., 2017).

The non-rigid pinna motions were divided further into two types: 'opening' and 'closing' motions. The definition for these two motion types was based on the distance between two landmark points on the anterior and posterior pinna rim, respectively (anterior: point number 4, posterior: point number 6; Fig. 3C). A decrease in the distance between points 4 and 6 was defined as a closing motion, an increase an opening motion.

The existence of a relationship between the noseleaf and pinna motions was tested by estimating: (i) the frequency of occurrence for rigid and non-rigid pinna motions that occurred during different noseleaf motion types, (ii) the frequency of occurrence for opening and closing pinna motions during different noseleaf motion types, and (iii) a canonical correlation analysis based on landmark motion trajectories simultaneously obtained for the noseleaves and pinnae.

The frequency of rigid and non-rigid pinna motions that were associated with each noseleaf motion category was estimated over the entire dataset (590 pinna motion sequences). These pinna motion sequences were grouped according to the noseleaf motion category they were associated with. A bootstrap dataset with 1000 data points was created by sampling the original data with replacement to assess the variability of the estimates.

The estimates for the frequency of opening and closing pinna motions that were associated with each noseleaf motion category were based on the same dataset as those for rigid and non-rigid pinna motions. The pinna motions associated with each noseleaf motion category were classified as either rigid, opening or closing according to the criteria described above. A *t*-test (with Bonferroni correction) was used to assess differences in the changes in the pinna aperture width that were associated with the different combinations of noseleaf and pinna motion types.

The strength of the relationships between the noseleaf and pinna motions was quantified using canonical correlation analysis (Hardoon et al., 2004). The analysis was based on the three-dimensional motion trajectories of all seven noseleaf landmark points and seven landmark points on each pinna. It finds the rotation of the original data coordinate system that maximizes the linear correlation between the dimensions. The analysis was carried out separately for each of the four different noseleaf motion categories (closing, opening, random, no motion) and was used to quantify the correlation between noseleaf motion and the motions of the left and right ears as well as between left and right ear motions.

RESULTS

The noseleaf kinematics recordings could be separated into four well-separated clusters (Fig. 4) that corresponded to the previously defined motion categories: closing, opening, random motions and no motion. All recorded closing motions coincided with the

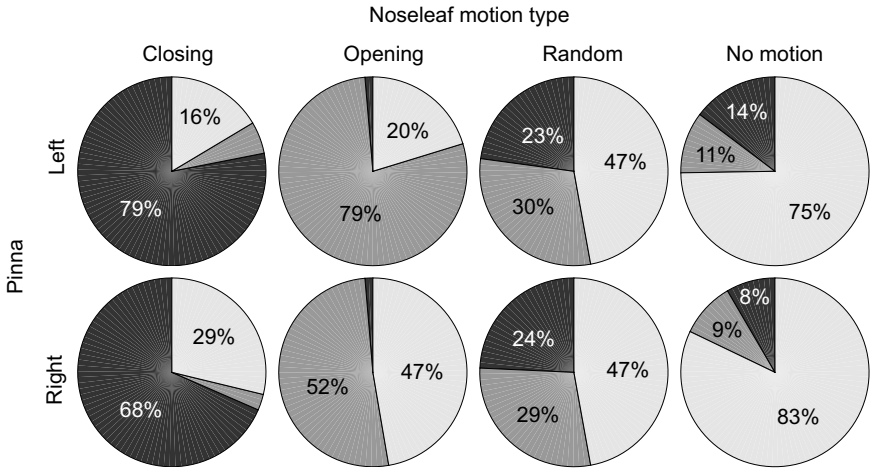

Fig. 6. Frequency of occurrence for different pinna motion patterns across the four noseleaf motion types. Pinna motion patterns are as follows: rigid motion, light gray; opening motion, dark gray; closing motion, black.

Journal of Experimental Biology (2019) 222, jeb210252. doi:10.1242/jeb.210252

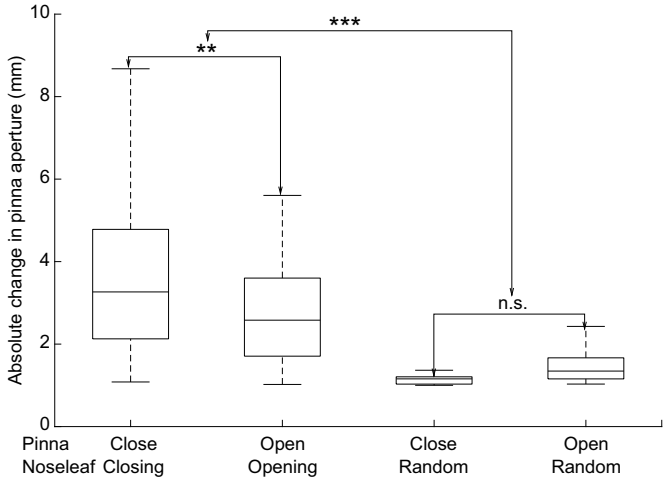

Fig. 7. Comparison of pinna deformation amplitude for different noseleaf and pinna motion types. Statistical significance levels: ***P<0.001; **P<0.01; n.s., not significant.

emission of biosonar pulses, whereas only three out of 74 analyzed opening motions did. Furthermore, these overlaps were only partial, with the final portion of the pulse overlapping with the initial portion of the opening motion. The random motions were characterized by initial opening states that tended to be larger than opening motion.

As predicted by a coordination of noseleaf and pinna motions, the relative frequency of rigid and non-rigid pinna motions differed greatly depending on the respective noseleaf motion type. Whereas closing and opening motions of the noseleaf were mostly accompanied by non-rigid pinna motions (68.95 to 90.41%), the random and no motion categories coincided mostly with rigid pinna motions (68.53 to 82.13%; Fig. 5). Left and right pinnae showed the same tendencies with moderate differences (up to 17.5% for the opening noseleaf motions).

When the non-rigid pinna motions were broken up into opening and closing motions, the relative frequencies of these categories were again dependent on the respective noseleaf motion (Fig. 6). Noseleaf and pinnae tended to open and close together. The pinna motions that co-occurred with different types of noseleaf motions also differed in their amplitudes. Pinna motions that were associated with closing and opening noseleaf motions were much larger than those associated with random motions (Fig. 7). Closing pinna motions occurring during closing noseleaf motions were also significantly larger than opening pinna motions occurring during opening noseleaf motions, but the distributions overlapped substantially (Fig. 7).

Finally, the results of canonical correlations analysis showed the relationship between the noseleaf and pinna deformations as predicted by a coordination between these motions (Fig. 8). The correlation coefficients ranged from 0.83 to 0.94 for all motion categories. In contrast to this, the correlation coefficients for the no motion recordings were 0.49 and 0.59 for the right and left pinna, respectively.

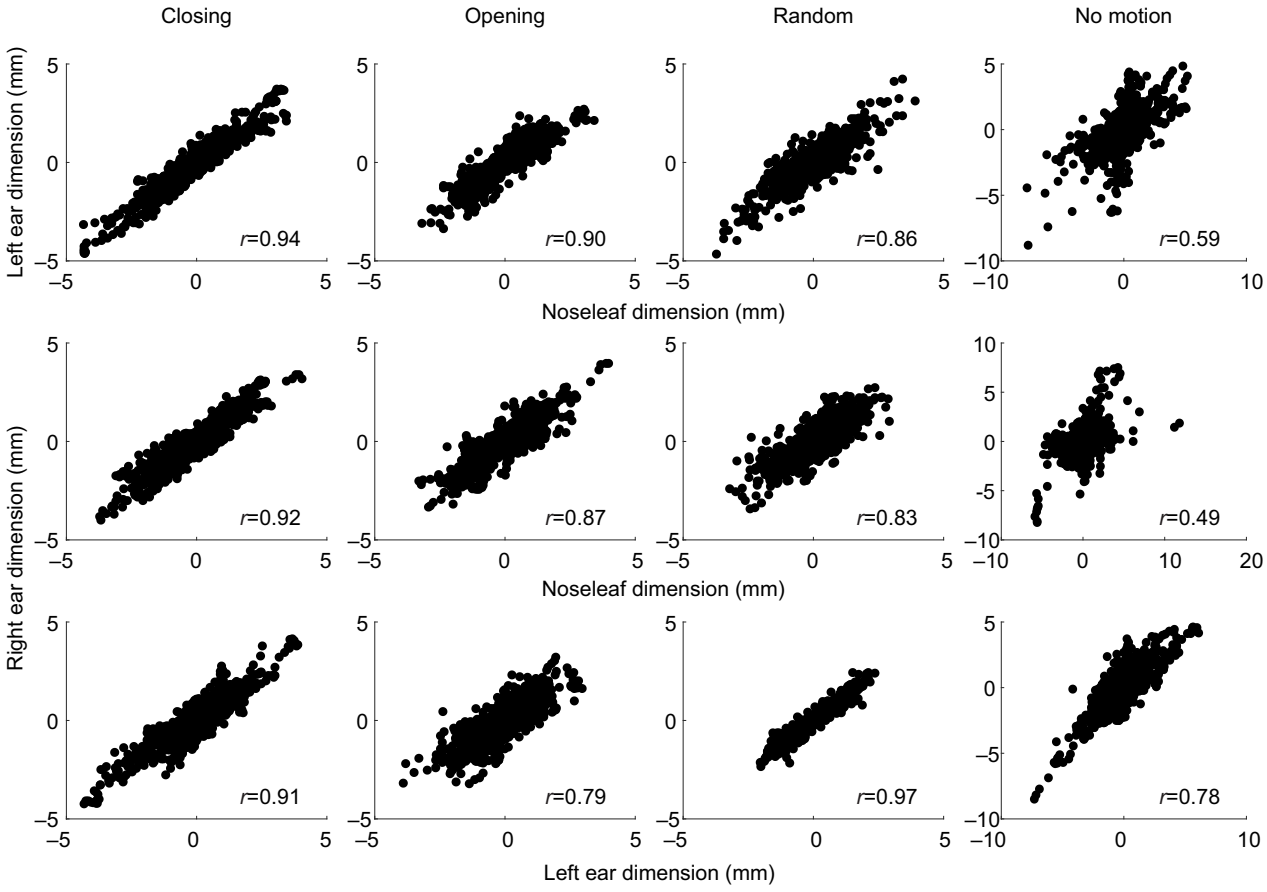

Fig. 8. Canonical correlation analysis results: relationship between noseleaf and left pinna motions (top row), between noseleaf and right pinna (middle row), and between left and right pinnae (bottom row). Each column corresponds to a different noseleaf motion type (closing, opening, random motion, and the no motion reference).

The motion of the landmark points on the left and right pinna were likewise found to be correlated with coefficients ranging between 0.87 and 0.97. The no motion category was no exception in this respect.

DISCUSSION

The qualitative and quantitative relationships demonstrated here are predicted by the hypothesis that the biosonar system of hipposiderid bats relies on synergistic integration of emission and reception dynamics. Especially the quantitative relationships between both pinnae and the noseleaf support the hypothesis that the bats have a fine coordination of the shape details of these three interface structures. The results obtained for the no motion category serve as an important reference, because they demonstrate that the observed correlations are not artifacts. The very weak correlations that were seen in the reference conditions could be due to small, overall head motions that had an effect on the noseleaf as well as the ears.

However, demonstrating relationships at the level of the motion kinematics is not sufficient proof for the existence of synergistic effects at the acoustic/functional level, nor does it show that the bats make use of these relationships. Hence, the next step in investigating this hypothesis further could be to look at possible functional advantages that the coordination of noseleaf and pinna motions could provide. Investigating this question could build upon the findings from the current work as it provides specific insights into the nature of coordination between these motions (e.g. noseleaf and pinna closing motions occur together). Further analysis could contrast coordinated motion patterns that are seen in bats against those that are not seen in bats in order to find differences of possible functional relevance.

Besides the hipposiderid bats studied here, other groups and species of bats also have biosonar emission and reception structures that could form a substrate for coordinated dynamics on both interfaces. Noseleaves, for example, are found not only in the hipposiderid bats and the closely related horseshoe bats, but also in the New World spear-nosed bats (family Phyllostomidae) and other small groups. Similarly, mouth-emitting bats could use their lips and appendages (e.g. in the ghost-faced bats, *Mormoops blainvillii* and *M. megalophylla*) to accomplish similar modulations of the emitted pulses. On the reception side, ear motions have been reported in vespertilionid species such as the big brown bat (*Eptesicus fuscus*; Valentine et al., 2002). Hence, mobility on the reception side may not be restricted to the bat groups that are known to have highly developed pinna musculatures. Instead, it could be that emitter and receiver dynamics and possibly coordination between the two can be found beyond hipposiderid bats.

If it is possible to assign functional relevance to a coordinated dynamics across the emission and reception side of biosonar in hipposiderid or other bats, these principles could also be of interest in research regarding man-made sonar sensing systems. At present, there is no direct equivalence to the non-rigid deformations of the bat noseleaves and pinnae in technical sonar. Introducing such dynamics would require decisions as to whether and how the dynamics in these structures should be coordinated. Taking a closer look at how bats coordinate their motions could help to integrate this novel, dynamic dimension into man-made technology.

Acknowledgements

The authors would like to thank Peter Windes for help with the canonical correlation analysis method. Song Wang, Shuqi Dong and Zijun Di helped with processing of the data.

Competing interests

The authors declare no competing or financial interests.

Author contributions

Conceptualization: S.Z., R.M.; Methodology: S.Z., R.M.; Software: S.Z., Y.L.; Validation: S.Z.; Formal analysis: S.Z., R.M.; Investigation: S.Z., Y.L., J.T., L.Y.; Resources: S.Z., Y.L., J.T., L.Y.; Data curation: S.Z., Y.L., J.T., L.Y.; Writing - original draft: S.Z.; Writing - review & editing: S.Z., R.M.; Visualization: S.Z., R.M.; Supervision: R.M.; Project administration: R.M.; Funding acquisition: R.M.

Funding

This work was supported through funding from the National Natural Science Foundation of China (grants 11374192, 11574183), the Fundamental Research Fund of Shandong University (grant 2014QY008) and a fellowship from the China Scholarship Council (grant 201806220156).

References

Bates, M. E., Simmons, J. A. and Zorikov, T. V. (2011). Bats use echo harmonic structure to distinguish their targets from background clutter. *Science* **333**, 627-630. doi:10.1126/science.1202065

Bouguet, J. Y. and Perona, P. (1998). Camera calibration from points and lines in dual-space geometry. In Proc. 5th European Conf. on Computer Vision (ed. H. Burkhardt and B. Neumann), pp. 2-6. Springer Science & Business Media.

Commins, S. (2018). *Behavioural Neuroscience*. Cambridge University Press.

Corcoran, A. J. and Moss, C. F. (2017). Sensing in a noisy world: lessons from auditory specialists, echolocating bats. *J. Exp. Biol.* **220**, 4554-4566. doi:10.1242/jeb.163063

Davies, K. T. J., Maryanto, I. and Rossiter, S. J. (2013). Evolutionary origins of ultrasonic hearing and laryngeal echolocation in bats inferred from morphological analyses of the inner ear. *Front. Zool.* **10**, 2. doi:10.1186/1742-9994-10-2

Feng, L., Gao, L., Lu, H. and Müller, R. (2012). Noseleaf dynamics during pulse emission in horseshoe bats. *PLoS ONE* **7**, e34685. doi:10.1371/journal.pone.0034685

Fu, Y., Caspers, P. and Müller, R. (2016). A dynamic ultrasonic emitter inspired by horseshoe bat noseleaves. *Bioinspir. Biomim.* **11**, 036007. doi:10.1088/1748-3190/11/3/036007

Fujita, K. and Kashimori, Y. (2016). Neural mechanism of corticofugal modulation of tuning property in frequency domain of bat's auditory system. *Neural Process. Lett.* **43**, 537-551. doi:10.1007/s11063-015-9425-6

Gao, L., Balakrishnan, S., He, W., Yan, Z. and Müller, R. (2011). Ear deformations give bats a physical mechanism for fast adaptation of ultrasonic beam patterns. *Phys. Rev. Lett.* **107**, 214301. doi:10.1103/PhysRevLett.107.214301

Gupta, A. K., Webster, D. and Müller, R. (2015). Interplay of lancet furrows and shape change in the horseshoe bat noseleaf. *J. Acoust. Soc. Am.* **138**, 3188-3194. doi:10.1121/1.4935387

Gupta, A. K., Webster, D. and Müller, R. (2018). Entropy analysis of frequency and shape change in horseshoe bat biosonar. *Phys. Rev. E* **97**, 062402. doi:10.1103/PhysRevE.97.062402

Hardoon, D. R., Szedmak, S. and Shawe-Taylor, J. (2004). Canonical correlation analysis: an overview with application to learning methods. *Neural Comput.* **16**, 2639-2664. doi:10.1162/0899766042321814

He, W., Pedersen, S. C., Gupta, A. K., Simmons, J. A. and Müller, R. (2015). Lancet dynamics in greater horseshoe bats, *Rhinolophus ferrumequinum*. *PLoS ONE* **10**, e0121700. doi:10.1371/journal.pone.0121700

Hedrick, T. L. (2008). Software techniques for two- and three-dimensional kinematic measurements of biological and biomimetic systems. *Bioinspir. Biomim.* **3**, 034001. doi:10.1088/1748-3182/3/3/034001

Hiryu, S., Katsura, K., Lin, L.-K., Riquimaroux, H. and Watanabe, Y. (2005). Doppler-shift compensation in the Taiwanese leaf-nosed bat (*Hipposideros terasensis*) recorded with a telemetry microphone system during flight. *J. Acoust. Soc. Am.* **118**, 3927-3933. doi:10.1121/1.2130940

Kössl, M. and Vater, M. (1995). Cochlear structure and function in bats. In *Hearing by Bats* (ed. A. N. Popper and R. R. Fay), pp. 191-234. New York, NY: Springer.

Likas, A., Vlassis, N. and Verbeek, J. J. (2003). The global k-means clustering algorithm. *Pattern Recognit.* **36**, 451-461. doi:10.1016/S0031-3203(02)00060-2

Matsuta, N., Hiryu, S., Fujioka, E., Yamada, Y., Riquimaroux, H. and Watanabe, Y. (2013). Adaptive beam-width control of echolocation sounds by CF–FM bats, *Rhinolophus ferrumequinum nippon*, during prey-capture flight. *J. Exp. Biol.* **216**, 1210-1218. doi:10.1242/jeb.081398

Metzner, W. and Müller, R. (2016). Ultrasound production, emission, and reception. In *Bat Bioacoustics* (ed. M. B. Fenton, A. D. Grinnell, A. N. Popper and R. R. Fay), pp. 55-91. New York, NY: Springer.

Mogdans, J., Ostwald, J. and Schnitzler, H. U. (1988). The role of pinna movement for the localization of vertical and horizontal wire obstacles in the greater horseshoe bat, *Rhinolopus ferrumequinum*. *J. Acoust. Soc. Am.* **84**, 1676-1679. doi:10.1121/1.397183

Moss, C. F. (2018). Auditory mechanisms of echolocation in bats. In *Oxford Research Encyclopedia of Neuroscience* (ed. S. M. Sherman). Oxford University Press. doi:10.1093/acrefore/9780190264086.013.102

Moss, C. F. and Sinha, S. R. (2003). Neurobiology of echolocation in bats. *Curr. Opin. Neurobiol.* **13**, 751-758. doi:10.1016/j.conb.2003.10.016

Müller, R., Gupta, A. K., Zhu, H., Pannala, M., Gillani, U. S., Fu, Y., Caspers, P. and Buck, J. R. (2017). Dynamic substrate for the physical encoding of sensory information in bat biosonar. *Phys. Rev. Lett.* **118**, 158102. doi:10.1103/PhysRevLett.118.158102

Neuweiler, G. (2000). *The Biology of Bats*. Oxford University Press on Demand.

Neuweiler, G., Metzner, W., Heilmann, U., Rübsamen, R., Eckrich, M. and Costa, H. H. (1987). Foraging behaviour and echolocation in the rufous horseshoe bat (*Rhinolophus rouxi*) of Sri Lanka. *Behav. Ecol. Sociobiol.* **20**, 53-67. doi:10.1007/BF00292166

Schneider, H. and Möhres, F. P. (1960). Die ohrbewegungen der hufeisenfledermäuse (Chiroptera, Rhinolophidae) und der mechanismus des bildhörens. *J. Comp. Physiol.* **44**, 1-40. doi:10.1007/BF00297861

Schnitzler, H.-U. (1968). Die ultraschall-ortungslaute der hufeisen-fledermäuse (Chiroptera-Rhinolophidae) in verschiedenen orientierungssituationen. *Z. Vergl. Physiol.* **57**, 376-408. doi:10.1007/BF00303062

Schnitzler, H.-U. (1973). Control of Doppler shift compensation in the greater horseshoe bat, *Rhinolophus ferrumequinum*. *J. Comp. Physiol.* **82**, 79-92. doi:10.1007/BF00714171

Simmons, J. A. and Stein, R. A. (1980). Acoustic imaging in bat sonar: echolocation signals and the evolution of echolocation. *J. Comp. Physiol.* **135**, 61-84. doi:10.1007/BF00660182

Simmons, J. A., Fenton, M. B. and O'Farrell, M. J. (1979). Echolocation and pursuit of prey by bats. *Science* **203**, 16-21. doi:10.1126/science.758674

Trappe, M. and Schnitzler, H.-U. (1982). Doppler-shift compensation in insect-catching horseshoe bats. *Naturwissenschaften* **69**, 193-194. doi:10.1007/BF00364902

Valentine, D. E., Sinha, S. R. and Moss, C. F. (2002). Orienting responses and vocalizations produced by microstimulation in the superior colliculus of the echolocating bat, *Eptesicus fuscus*. *J. Comp. Physiol.* **188**, 89-108. doi:10.1007/s00359-001-0275-5

Walker, V. A., Peremans, H. and Hallam, J. C. T. (1998). One tone, two ears, three dimensions: a robotic investigation of pinnae movements used by rhinolophid and hipposiderid bats. *J. Acoust. Soc. Am.* **104**, 569-579. doi:10.1121/1.423256

Yin, X., Qiu, P., Yang, L. and Müller, R. (2017). Horseshoe bats and old world leaf-nosed bats have two discrete types of pinna motions. *J. Acoust. Soc. Am.* **141**, 3011-3017. doi:10.1121/1.4982042

Yu, C., Luo, J., Wohlgemuth, M. and Moss, C. F. (2019). Echolocating bats inspect and discriminate landmark features to guide navigation. *J. Exp. Biol.* **222**, jeb191965. doi:10.1242/jeb.191965